EUV Performance of a Multilayer Coated High-Density Toroidal Grating

Ritva A. M. Keski-Kuha, Roger J. Thomas, Werner M. Neupert,
Charles E. Condor, Jeffrey S. Gum

NASA/ Goddard Space Flight Center
Greenbelt, Maryland 20771

Abstract

Performance of a multilayer coated diffraction grating has been evaluated in the EUV. The application of a multilayer coating to a blazed toroidal grating of high ruling density has produced a significant enhancement in grating efficiency in the 30 nm spectral region in first order and has maintained the excellent quasi stigmatic spectral resolution of the grating.

Introduction

The development of multilayer coatings with enhanced normal incidence reflectance allows us to take advantage of the conventional normal incidence mirror technology in the EUV. An extensive amount of work has already been done on applying multilayer coatings to mirrors both for laboratory applications and for astronomical applications in sounding rocket experiments[1-10]. It would also be desirable to apply this technology to diffraction gratings in order to provide enhanced efficiency for normal incidence spectrographs in wavelength regions where only glancing incidence designs have provided acceptable throughput in the past.

The application of multilayer coatings to diffraction gratings for use in the spectral region below 20 nm has been studied by several investigators[11-15]. They have demonstrated that multilayer coatings can provide gratings with enhanced efficiency over a narrow bandpass. Enhancement has also been demonstrated in the 30 nm spectral region for a sinusoidal grating[3]. This paper discusses the application of a multilayer coating to a large, concave, aspheric diffraction grating, a 3600 1/mm toroidal blazed replica, designed for operation in the 30 nm spectral region in first order.

Grating Characteristics

The grating coated for this study was originally developed for the Solar EUV Rocket Telescope and Spectrograph (SERTS) instrument[16]. The optical concept of that instrument uses a grazing incidence Wolter type 2 telescope to feed a quasi stigmatic spectrograph, in which the toroidal grating operating near normal incidence acts to re-image a spectrally dispersed version of the solar image falling onto its entrance aperture. The measured optical parameters for the SERTS master grating are shown in Table 1.

Table 1: SERTS grating parameters.

Substrate material:	Zerodur
Dimensions:	95 mm x 85 mm
Optical surface shape:	Toroid (prolate spheroid)
Dispersion radius (R_t):	1209.67 mm
Cross radius (R_s):	1200.02 mm
Radius ratio (R_s/R_t):	0.9920
Surface figure error:	40 nm (p-v)
Ruling frequency:	3600 l/mm
Ruling width:	65 mm
Ruling length:	80 mm
Grating blaze:	2.8° (tri-partite)
Coating:	Gold

The high-quality concave toroidal shape of the master grating's optical surface was polished directly into the Zerodur substrate by Capricorn Optical Corp. In addition to standard comparisons against a spherical test plate, measurements of the toroid's two radii of curvature, and of the surface figure error, were made optically in visible light during this polishing procedure with a Laser Unequal Path Interferometer (Figure 1). The measurement takes advantage of the fact that such toroidal surfaces produce stigmatic imaging in zero order when operated in a special configuration that has a known relationship to the surface parameters. In this configuration, the laser source is focussed through a point to illuminate the toroidal grating, which produces an image of the source point in zero order. A precision polished sphere centered on the grating image point then sends the beam back through the optical train, so that the interferometer can compare the outgoing and returning wavefronts. After the system is adjusted to minimize the measured wavefront differences, the distance from the source to image point (2*L) and the perpendicular distance from the source-image line to the grating vertex (D) are related to the grating blank's two radii of curvature as follows:

$$R_s = D \ , \qquad R_t = (L^2 + D^2) \ / \ D \ .$$

The residual wavefront differences are then a direct measurement of the figure error in the toroidal surfaces in units of the source laser wavelength. This procedure is particularly sensitive in that the test beam is modulated twice by a given point on the grating surface for each measurement.

The master was ruled and gold coated at Hyperfine Inc., which also made several replicas from it by means of a convex toroidal submaster and concave toroidal

replica blanks. The gratings were then tested for EUV efficiency at the Synchrotron Ultraviolet Radiation Facility (SURF-II) of the National Institute of Standards and Technology (NIST) in Gaithersburg, Maryland. Their spectral resolutions were also measured in a Spectrograph Test Chamber developed for that purpose by the Solar Physics Branch at GSFC. These measurements were used to select the best replica for flight on the SERTS experiment. The grating chosen for the multilayer study described here was one of the flight spare replicas from this group. It had no special processing to prepare it for the multilayer coating procedure.

Coating Process

The coating selected for the grating was a 10-layer Ir/Si multilayer optimized for 30.4 nm with a calculated reflectance of 21% at normal incidence at 30.4 nm. The optical constants used in the calculations are reported in Refs. 17, 18 for Ir films and Refs. 19, 20, 21 for Si films. The multilayer coating starting with silicon, was deposited directly on the gold base coating using e-beam evaporation in a 2-m diameter evaporator[22] at GSFC. Four 5x5 cm microscope slides were mounted next to the grating. The grating and the microscope slides were located 83 cm above the source, and the center of the grating was off-set 9 cm from the center of the source. Based on distribution studies, the layer thickness uniformity across the grating was about 2%. The EUV reflectances of the microscope slide coatings were measured using a reflectometer/monochromator system described elsewhere[23]. At a 15° angle of incidence, the 30.4 nm reflectance varied from 15.0% to 15.3% on the four microscope slides with the slide located farthest away from the source having the highest reflectance. The 30.4 nm reflectance of that coating increased to 16.1% at a 12° angle of incidence, which is the smallest angle that can be measured due to instrument limitations.

Grating Test Procedure and Results

Efficiency

SURF-II is a synchrotron ultraviolet radiation facility operated by the Center for Radiation Research, National Measurement Laboratory at the National Institute of Standards and Technology (NIST). It provides a highly characterized national radiometric standard throughout the XUV spectral range, with an overall accuracy of about two percent as determined by inter comparison with a variety of transfer standards. The radiation produced is highly plane polarized XUV continuum that emerges in a narrow, roughly collimated beam. Of the several beamlines available, our grating measurements were carried out on Beamline 2, which has been designated as a spectrometer calibration beamline and is under the partial sponsorship of NASA. The measurements reported here were made at the first of the two calibration stations on Beamline 2, located 11.5 m from the storage ring tangent point. It has provisions for precision controlled two axis translation and rotation, permitting accurate angular alignment and sub-aperture mapping over the grating's ruled area.

The principal features of our grating calibration chamber are shown in Figure 2. The chamber is first aligned to the synchrotron beam in visible light by means of a reference mirror attached to its rear wall. Then the test grating is installed at its normal operating angle of 7.0° and the chamber is evacuated. When the SURF-II beam is allowed to illuminate the grating, its alignment can be verified by the location of the visible zero-order spot seen on the side viewing port window. Pitch scans can also be performed to assure that the detector is properly centered relative to the dispersion plane. The diffracted EUV beam falls onto an exit slit

2.0 mm wide by 9 mm long placed in front of a windowless photodiode whose EUV response versus wavelength has been independently calibrated by NIST personnel. The output of the photodiode is determined by an electrometer, which is itself independently recalibrated as needed.

The exit slit and photodiode are mounted on an arm that pivots about an axis passing through the grating's vertex and perpendicular to its dispersion plane. The position of the arm is controlled from outside the vacuum chamber through a mechanical linkage, and is measured by reading an odometer type dial on the arm gearing. This allows tests of the grating efficiency over the full wavelength range of about 20 - 60 nm. The conversion between arm readings and a wavelength scale was determined by geometrical considerations, and is checked periodically by carrying out measurement runs that include appropriate 'edge' filters. For that purpose, thin filters of Ge and Sn/Ge are occasionally placed in the beam to introduce discontinuities at known wavelengths in the otherwise smoothly varying EUV continuum distribution, thus providing identifiable wavelength fiducials.

The size of the SURF-II beam is defined by a 13 mm circular aperture that is 10.538 m from the synchrotron tangent point. The grating being tested is located 11.922 m from the tangent point, and so the instantaneously illuminated area is 14.7 mm in diameter. During a measurement run, the chamber is translated in a rectangular pattern of 17.7 mm increments so that a total of nine sub-aperture surface positions are mapped. Due to length limitations, the distance from the grating vertex to the exit slit is only 55 cm, instead of the true focal distance of 63.67 cm for the SURF test configuration as determined by ray-trace calculations. Thus, the size of a diffracted spot of a given wavelength at the exit slit is:

$$14.7 \times (63.67 - 55) / 63.67 = 2.0 \text{ mm},$$

which sets the lower limit on the useful width of the exit slit. Since the spectral dispersion at that distance is 0.505 nm/mm, the FWHM of the detector's response for each position setting is 1.01 nm.

Along with readings of the dial indicator for the detector arm position and electrometer values for the photodiode output, the synchrotron beam current is recorded at the beginning and end of the wavelength scans for each of the nine grating locations illuminated. For the beam conditions on that day, this allows a determination of the exact incident flux as a function of wavelength from tables supplied by the SURF-II operators.

A SERTS flight spare replica grating, serial number 605-12-1, with a standard gold coating was tested in this way at NIST. The grating was then overcoated with a 10-layer Ir-Si multilayer optimized for 30.4 nm, as described above, and remeasured in the grating evaluation chamber at NIST. The absolute efficiency at each of the nine measured positions before and after application of the multilayer coating are shown in Figure 3. The ratio of efficiencies combined from all positional measurements is given in Figure 4. At the shorter wavelengths, the individual efficiencies were low enough to cause some scatter in the ratio values, but at longer wavelengths the ratio seems to be remarkably uniform over the nine different locations on the grating.

These measurements show that the multilayer coating gave an efficiency enhancement that peaked very close to 30 nm, where the grating's first order effciency increased from 0.48 % to 3.5 %, more than a factor of 7 above that of the standard gold

coating. This represents the highest reflectance at that wavelength yet reported for a high-resolution grating operating at near normal incidence, to our knowledge. The multilayer coating provided some enhancement over the entire 10 nm band from 25 to 35 nm, and at least a factor of 4 enhancement over the 6 nm band from 26.5 to 32.5 nm. These bandpasses are well matched to spectrograph designs that use two dimensional array detectors, such as EUV sensitive CCDs, whose active dimensions can be as large as 1 or 2 cm. With a number of pixels on the order of 1000, such a system could provide a spectral resolution of about 5000 over a bandpass of more than 40 nm at EUV wavelengths with high sensitivity, if the multilayer coating itself does not significantly degrade the spectral performance of the toroidal grating.

Spectral resolution

To test that possibility, we made before and after measurements of the grating's spectral resolution in the SERTS Spectrograph Test Chamber at GSFC. This facility allows the spectrograph section of the SERTS rocket instrument itself (shown in Figure 5) to be attached to a vacuum system provided with a hollow cathode gas flow EUV light source. The light source uses a combination of Helium and Neon gases to produce a large number of spectral lines throughout the EUV wavelength range of interest. Radiation from the source lamp is concentrated onto the spectrograph entrance aperture by means of a grazing incidence ellipsoidal mirror to increase the system's speed. The resultant images are recorded on Kodak Special Film, Type 101-07, which has been specifically developed for sensitivity in the EUV. Since the spectrograph's entrance aperture, Aluminum filter, toroidal grating, and film camera can all be flight units, this arrangement permits the final alignment and focus adjustments to be made on the SERTS optical components, as well as providing the pre- and post-flight instrumental performance parameters directly in the EUV wavelengths of interest.

For the tests reported here, the original resolution measurements were made on the toroidal grating that was used in the two most recent flights of the SERTS rocket experiment, as a part of their pre- and post-flight calibrations. At that time, the grating selected for flight (serial number 605-10-1) demonstrated a similar, but slightly better, performance than its replica-mate (605-12-1). After the flight-spare grating was coated with the 10-layer Ir/Si multilayer, and after its EUV reflectance was remeasured at NIST, it was substituted for the SERTS-3 flight grating in the Spectrograph Test Chamber and a total of seven EUV exposures of various durations were made in a single configuration run. It should be noted that there was no attempt to fine tune the multilayer grating's alignment or EUV focus, and therefore the results may be somewhat less than optimized.

The spectrograph entrance aperture is made up of two parts, a narrow slit near the instrument's imaging axis, and a wider slot or 'lobe' on each end of the slit, as shown schematically in Figure 6. The quasi-stigmatic operation of the toroidal grating acts to produce spectrally dispersed images of this entrance aperture along the spectrograph's focal surface in the EUV emission lines of the illuminating source, thus providing both spectral and spatial information at wavelengths from roughly 24 to 45 nm. The present design parameters of the SERTS spectrograph, and therefore of the Spectrograph Test Chamber, are given in Table 2. Although this design is strictly stigmatic at only two specific wavelengths, the system's sagittal and tangential focii are sufficiently close over the full spectral range that the resultant spot sizes are determined almost entirely by factors other than limitations in theoretical performance.

Table 2: SERTS spectrograph parameters.

Grating dispersion radius (R_t):	1209.67 mm	
Grating cross radius (R_s):	1200.02 mm	
Grating ruling frequency:	3600 mm-1	
Grating operating angle:	7.01°	
Object distance:	1150 mm	
Average image distance:	1265 mm	
Spatial image magnification:	1.10	
Spectral dispersion:	0.22 nm/mm	
Physical length of spectrum:	97.3 mm	
Spectral range:	23.5 - 44.9 nm	
Narrow slit width:	13 μm (SERTS-2),	15 μm (SERTS-3)
Narrow slit length:	1.7 mm " ,	3.0 mm "
Lobe slot width:	0.5 mm " ,	3.0 mm "
Lobe slot length:	4.5 mm " ,	5.0 mm "

Figure 7 shows a representative post-flight spectrum taken on 1 November 1989 with the SERTS-3 replica grating (605-10-1) and entrance aperture, as compared to one taken on 4 January 1990 in the identical spectrograph chamber but with the backup replica grating (605-12-1) and its multilayer coating. The enhanced strength of the recorded lines around 30 nm is clearly seen in the multilayer spectrum. The two spectra are shifted relative to one another by .77 nm in wavelength, so that the strong line at the far right of the upper spectrum falls outside of the observed range of the lower one. This suggests that the operating angle of the multilayer grating was tilted by about 5 arcmin relative to the SERTS flight grating. Ray-trace calculations indicate that, without a corresponding focus correction, such a tilt could cause the theoretical (zero-slit) spot diameter in the spectral dimension to increase from the average aligned value of 0.4 pm (physical size of 1.9 μm) to as much as 1.5 pm (6.9 pm) in the misaligned case.

Spectral traces at a number of EUV wavelengths are shown in Figure 8, which compares the resolution of the multilayer coated grating (605-12-1) with the measurements made prior to the SERTS-2 and SERTS-3 rocket flights using grating 605-10-1. Clearly, the excellent spectral imaging properties of the grating have not been degraded by the multilayer coating or by the process of applying it. The average line widths (FWHM) measured for the five strongest unblended lines seen in Figure 8 (Ne II at 32.46, 32.65, 32.68, 32.76 and 32.81 nm) are given in Table 3. The small differences are well within the expected variations due to errors in focussing or alignment, or due to differences in the widths of the slits used in the measurements.

Table 3: Measured spectral performance.

Grating	Imaged Slit Width (μm)		Averaged EUV Line FWHM		Spectral Resolution at 32 nm
	Spectrom.	Microdens.	Linear (μm)	Spectral (pm)	
605-10-1 SERTS-2	14.3	2.5	21 ± 2	4.7 ± .4	6800
605-10-1 SERTS-3	16.5	3.3	36 ± 2	8.0 ± .5	4000
605-12-1 Multilayer	16.5	2.5	27 ± 1	6.0 ± .1	5300

Conclusions

In summary, the application of a multilayer coating to a large, high-density, aspheric diffraction grating replica has produced a significant enhancement in first-order efficiency over more than a 6 nm spectral band at wavelengths around 30 nm. This implies that a considerable improvement in throughput can be achieved in EUV instruments like SERTS that use gratings at normal incidence. The studies carried out to compare the spectral performance for the SERTS flight-spare grating before and after depositing the multilayer coating demonstrate that the grating suffered no loss in its excellent spectral resolution due to the coating process.

References

1. E. Spiller, "Reflective Multilayer Coatings for the Far UV Region", Appl. Opt. 15, 2333 (1976).
2. J.H. Underwood, and T.W. Barbee, "Layered Synthetic Microstructures as Bragg Diffractors for X Rays and Extreme Ultraviolet: Theory and Predicted Performance", Appl. Opt. 20, 3027 (1981).
3. R.A.M. Keski-Kuha, "Layered Synthetic Microstructure Technology Considerations for the Extreme Ultraviolet", Appl. Opt. 23, 3534 (1984).
4. T.W. Barbee, S. Mrowka, and M.C. Hettrick, "Molybdenum-Silicon Multilayer Mirrors for the Extreme Ultraviolet", Appl. Opt. 24, 883 (1984).
5. J. F. Meekins, R. G. Cruddace, and H. Gursky, "Optimization of Layered Synthetic Microstructures for Narrowband Reflectivity at Soft X-ray and EUV Wavelengths", Appl. Opt. 25, 2757 (1986).
6. J. F. Lindblom, A. B. C. Walker Jr., R. B. Hoover, T. W. Barbee Jr.,R. A. van Patten and J. P. Gill, "Soft X-Ray/Extreme Ultraviolet Images of the Solar Atmosphere with Normal Incidence Multilayer Optics," X-Ray Instrumentation in Astronomy II, Proc. SPIE 982, 316 (1988).
7. B. M. Haisch, T. E. Whittmore, E. G. Joki, W. J. Brookover and G. J. Rottman, "A Multilayer X-Ray Mirror for Solar Photometric Imaging Flown on a Sounding Rocket," X-Ray Instrumentation in Astronomy II, Proc. SPIE 982, 38 (1988).
8. R. C. Catura and L. Golub, "XUV Multilayered Optics for Astrophysics," Revue Phys. Appl. 23, 1741 (1988).
9. A.B.C. Walker, T.W. Barbee, R.B. Hoover, and J.F. Lindblom, "Soft X-Ray Images of the Solar Corona with a Normal Incidence Cassegrain Multilayer Telescope", Science 241, 1781 (1989).
10. L. Golub, M. Herant, K. Kalata, I. Lovas, G. Nystrom, F. Pardo, E. Spiller, and J. Wilczynski, "Sub-arcsecond Observations of the Solar X-ray Corona", Nature 344,

842 (1990).
11. J.C. Rife, W.R Hunter, T.W. Barbee and R.G. Cruddace, "Multilayer-coated Blazed Grating Performance in the Soft X-ray Region", Appl. Opt. 28, 2984 (1989).
12. T.W. Barbee, "Combined Microstructure X-Ray Optics", Rev. Sci. Insrum. 260, 1588 (1989).
13. J.C. Rife, T.W. Barbee, W.R. Hunter and R.G. Cruddace, "Performance of a Tungsten/Carbon Multilayer-coated Blazed Grating from 150 to 1700eV", Physica Scripta 41, 418 (1990).
14. R.G.Cruddace, T.W. Barbee, J.C. Rife and W.R. Hunter, "Measurements of the Normal-Incidence X-ray Reflectance of a Molybdenum-Silicon Multilayer Deposited on a 200 l/mm Grating", Physica Scripta 41, 396 (1990).
15. J.V. Bixler, T.W. Barbee and D. D. Dietrich, "Performance of Multilayer Coated Gratings in the Extreme Ultraviolet", X-Ray/EUV Optics for Astronomy and Microscopy, Proc. SPIE 1160, 648 (1989).
16. W.M. Neupert, G.L. Epstein, R.J. Thomas, and U. Feldman, "A Solar Ultraviolet Telescope and Spectrograph for Shuttle/Spacelab", Space Science Reviews 29, 425 (1981).
17. G, Hass, G.F. Jacobus, and W.R. Hunter, "Optical Properties of Evaporated Iridium Films in the Vacuum Ultraviolet from 500Å to 2000Å", J. Opt. Soc. Am. 57, 758 (1967).
18. J. F. Osantowski, NASA/Goddard Space Flight Center, private communication.
19. W.R. Hunter, in "Optical Properties and Electronic Structure of Metals and Alloys", F. Abeles Ed., p.136 (North Holland, Amsterdam, 1966).
20. W.R. Hunter, "On the Optical Constants of Metals at Wavelengths Shorter than their Critical Wavelength", J. Phys., Paris, 25, 154 (1964).
21. W.R. Hunter, Sachs-Freeman Associates private communication.
22. A.P.Bradford, G. Hass, J.F. Osantowski, and A.R. Toft, "Preparation of Mirror Coatings for the Vacuum Ultraviolet in the 2-m Evaporator", Appl. Opt. 8, 1183 (1969).
23. J.F. Osantowski, "Reflectance and Optical Constants for Cer-Vit from 250 to 1050Å", J. Opt. Soc. Am. 64, 834 (1974).

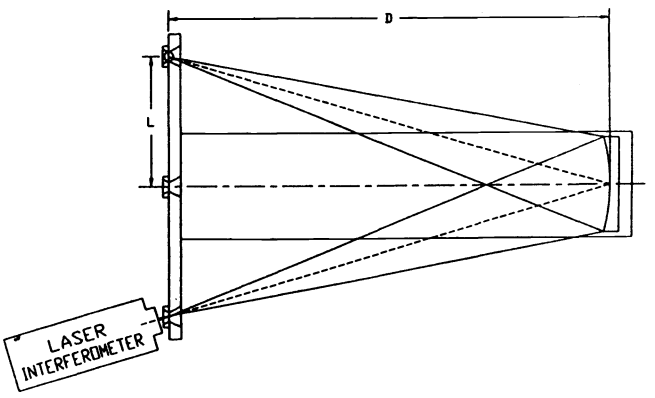

Figure 1. Test set-up for toroidal grating blanks.

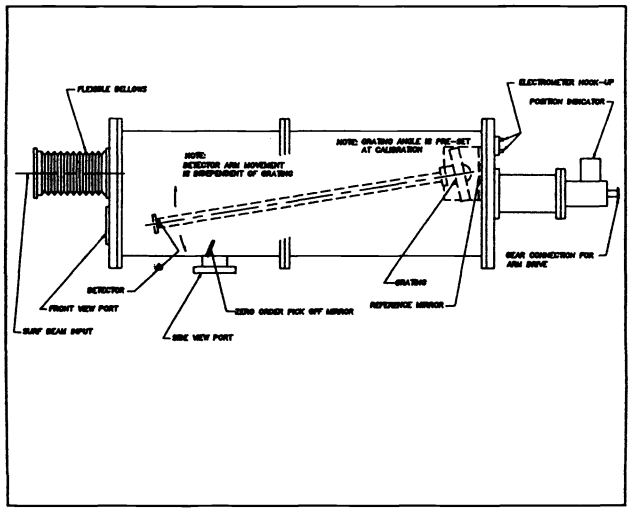

Figure 2. NIST grating evaluation chamber.

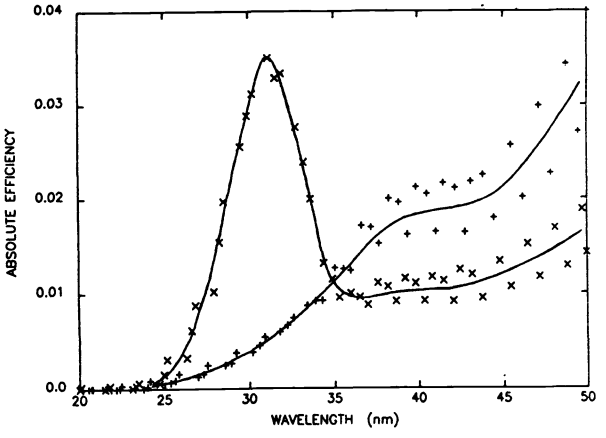

Figure 3. Absolute EUV efficiency before and after multilayer coating.

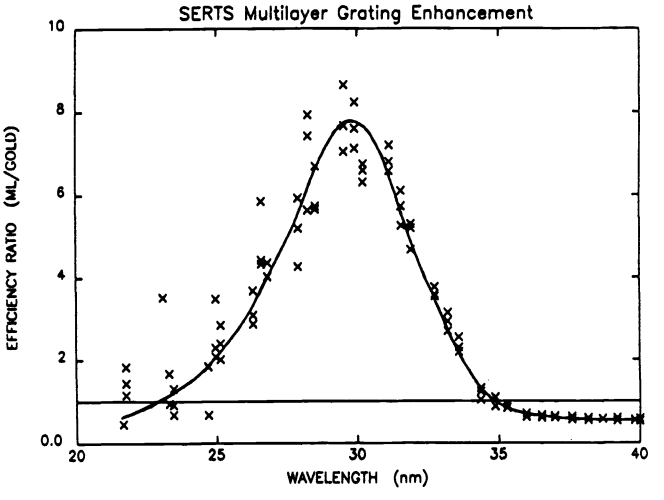

Figure 4. Enhancement in first-order EUV efficiency for the SERTS multilayer coated grating.

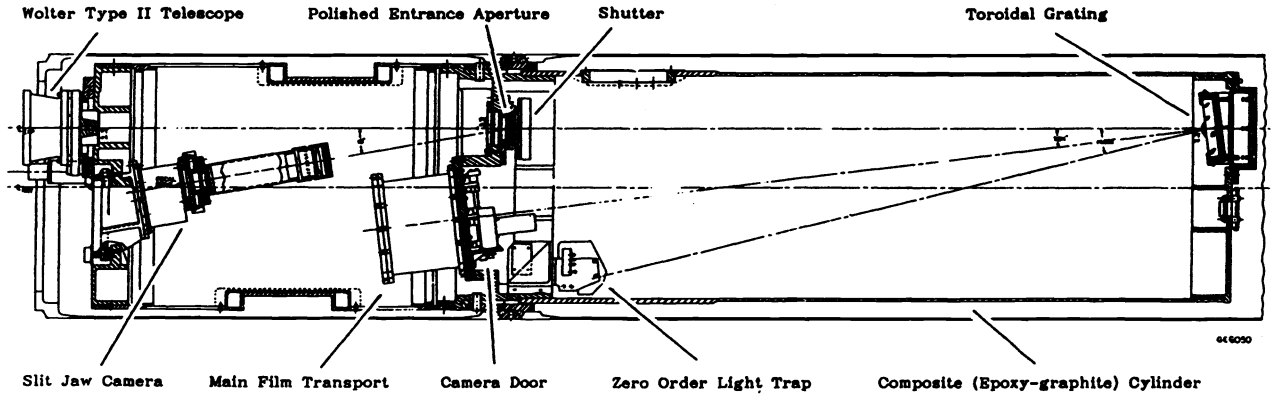

Figure 5. The Solar EUV Rocket Telescope and Spectrograph (SERTS).

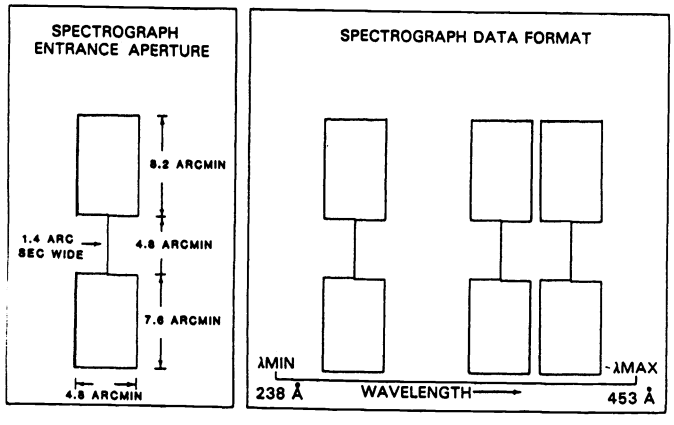

Figure 6. Layout of the SERTS spectrograph entrance aperture.

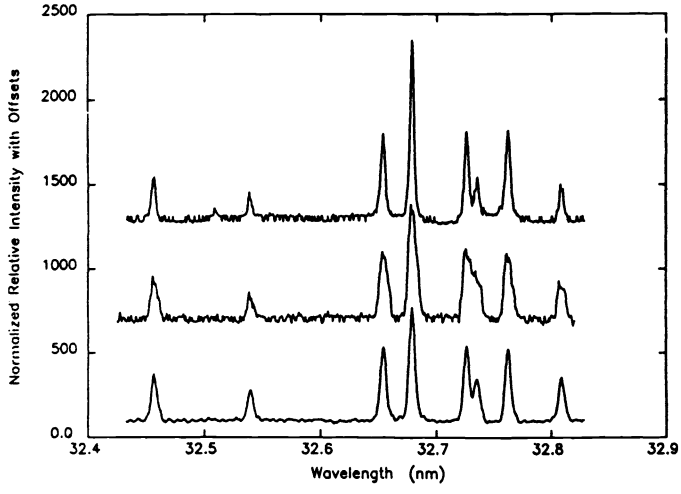

Figure 7. EUV Ne/He spectra produced with a gold coated grating (top) and with a multilayer coated grating (bottom).

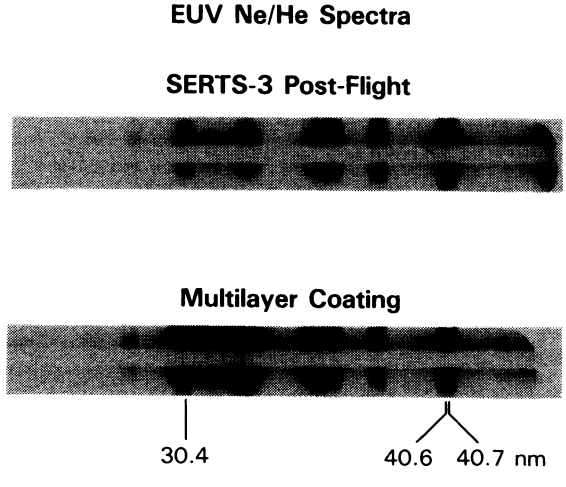

Figure 8. Microdensitometer traces of EUV Ne II spectra produced with a gold coated grating (top and middle) and with a multilayer coated grating (bottom).